

Atomic Modulation of Interdiffusion at Au-GaAs Interfaces

L. J. Brillson

Xerox Webster Research Center, Webster, New York 14580

and

G. Margaritondo and N. G. Stoffel

Department of Physics, University of Wisconsin, Madison, Wisconsin 53706

(Received 5 November 1979)

Monolayer thicknesses of Al are observed at Au-GaAs(110) interfaces modulate the relative Ga to As diffusion into Au by over an order of magnitude. This new phenomenon at compound semiconductor/metal interfaces reveals a systematic relationship between the local atomic bonding and the extended chemical structure of the interface.

The movement of semiconductor and metal atoms across a metal-semiconductor (M-SC) interface is a widely investigated phenomenon.¹ This interdiffusion is of particular significance for compound semiconductors¹ such as GaAs (Ref. 2) because it correlates with changes in interface electronic properties. The preferential diffusion of one constituent out of the semiconductor lattice can produce electrically active defects with energy levels in the band gap. Along with new states produced by metal diffusion into the semiconductor, these interface features strongly influence the Schottky barrier (SB) formation. Several ultrahigh-vacuum (uhv) studies of M-SC interfaces have recently emphasized the dominant influence of microscopic M-SC bonding in determining SB heights.³⁻⁵ For interfaces exhibiting no strong chemical reaction,³ significant interdiffusion can take place, the initial stages of which have recently been studied for Au on GaAs(110) by soft-x-ray photoemission spectroscopy (SXPS).^{5,6} In this Letter, we describe the dramatic effect which reactive monolayers of Al at the Au-GaAs(110) interface have on the macroscopic diffusion of Ga and As from the semiconductor crystal into a metallic Au overlayer. Specifically, the ratio of Ga to As outdiffusion increases systematically over an order of magnitude as the Al interface layer varies from fractions of a monolayer to several monolayers. This novel phenomenon demonstrates that microscopic interfacial bonding plays a central role in forming the macroscopic chemical composition and thereby the electronic structure of M-SC junctions.

SXPS experiments were carried out at the University of Wisconsin Synchrotron Radiation Center in a uhv chamber (base pressure $p = 5 \times 10^{-11}$ Torr). GaAs single crystals (Laser Diode, $n = 3.2 \times 10^{17}$ Te) were cleaved in uhv to expose (110) surfaces, onto which were evaporated thin Au and Al films. Metal deposition was monitored

by a quartz-crystal oscillator positioned next to the cleaved surface. Pressure rise during evaporation was in the 10^{-10} -Torr range. Spectra of Ga 3*d*, As 3*d*, Al 2*p*, and Au 4*f* core levels were obtained at $h\nu = 130$ and 80 eV with a cylindrical mirror analyzer (CMA). The CMA cylindrical axis was at 45° to the cleaved (110) surface normal and at 78° to the incident light beam. Overall energy resolution was 0.3 eV. Al coverages were also checked from the ratio of Al 2*p* to Ga 3*d* integrated core-level intensities at $h\nu = 130$ eV ($\text{Al}_{130}^{2p}/\text{Ga}_{130}^{3d}$) as calibrated previously.⁷ The core-level intensities reported here are integrated peak areas normalized to photon beam intensity and with a conventional background subtraction. For a given crystal cleavage, all intensities correspond to the same visually smooth areas of the cleaved surface.

Figure 1 illustrates Ga 3*d*, As 3*d*, and Al 2*p* core-level spectra taken at $h\nu = 130$ eV. The kinetic energies of all three core levels lie in the range corresponding to minimum escape depth ($\sim 4-6 \text{ \AA}$),⁸ thus giving maximum surface sensitivity which is further enhanced by the oblique collection geometry. The Al 2*p* core levels exhibit only one chemically shifted peak which does not vary with Au overlayer coverage. The absence of a "metallic" Al 2*p* peak at > 0.7 eV lower bonding energy demonstrates that the Al-GaAs surface bond does not dissociate with Au deposition and that no Al island formation takes place.⁹ A metallic-core-level feature does appear for 10 \AA Al on GaAs(110). Likewise, Au exhibits no metallic-core-level features below 4- \AA coverages but rather reduced 5*d* splittings and increased 4*f* binding energies characteristic of dispersed Au atoms.⁵ This indicates the absence of Au island formation.

Figure 1 shows that the ratio of Ga to As core-level intensities increases with Al deposition. For 8 \AA Au over 0.4 \AA Al on cleaved GaAs(110),

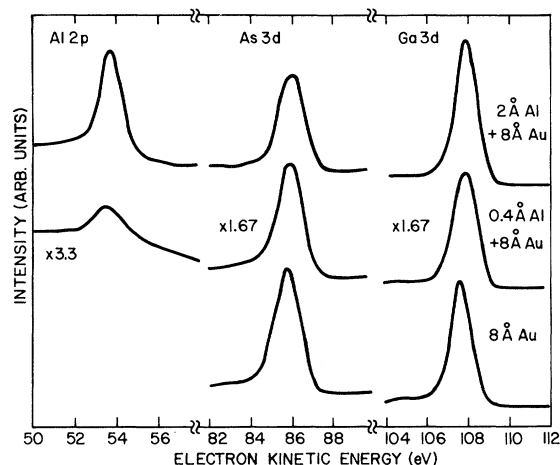


FIG. 1. Ga $3d$, As $3d$, and Al $2p$ core-level spectra vs Al interface coverage for 8 Å Au on cleaved GaAs(110). Background not subtracted.

the Ga $3d$ peak broadens by $>20\%$ while the As $3d$ peak exhibits no significant change. This broadening is due to a shift to lower binding energy corresponding to free Ga.⁹ For 8 Å over 2 Å Al on cleaved GaAs(110), the change in Ga $3d$ vs As $3d$ peak intensities relative to the cleaved surface is even more pronounced. Core-level spectra obtained with $h\nu = 80$ eV display still greater changes in the relative Ga $3d$ to As $3d$ intensities due to the higher surface sensitivity at Ga $3d$ kinetic energies (i.e., 58 eV). This indicates some accumulation of Ga near the metal-vacuum interface versus a more uniform As distribution throughout the Au. Furthermore, the $Ga^{3d}_{130}/Al^{2p}_{130}$ and $As^{3d}_{130}/Al^{2p}_{130}$ ratios first decrease and then increase with Au coverage, indicating both Au diffusion past Al into the GaAs and Ga and As outdiffusion into the Au. Thus the ability to tune the energy of the high-flux, synchrotron light source to achieve maximum surface sensitivity and detectability allows diffusion to be analyzed on an extremely fine scale.

Figure 2 illustrates how the $Ga^{3d}_{130}/As^{3d}_{130}$ ratio changes with Au deposition. For Au on cleaved GaAs(110) (i.e., 0 Å Al), the ratio decreases by 50% after 40 Å of Au deposit. A significant change in behavior occurs for the smallest increment of Al coverage—0.2 Å (0.15 GaAs monolayer). With increasing Al deposition, the GaAs nonstoichiometry on the outer surface becomes more pronounced. For the 2 Å Al versus 0 Å Al curves, the stoichiometry at 40 Å changes by a factor of 5. An order of magnitude change results from a 10-Å Al deposit. For this coverage, we also ob-

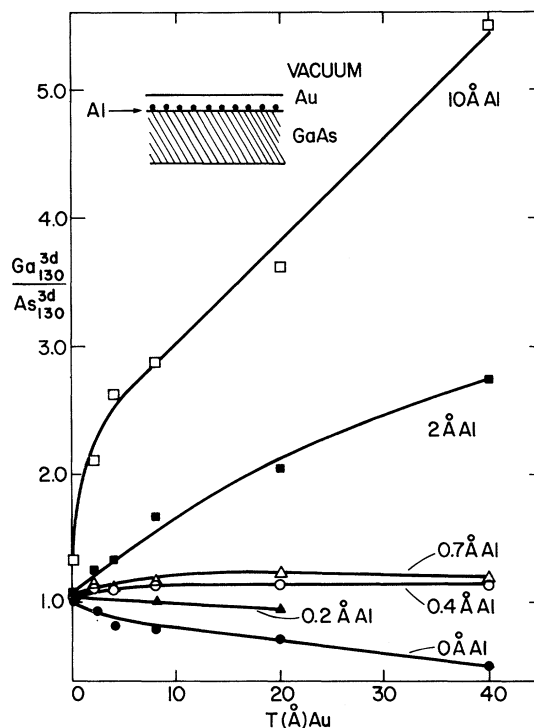


FIG. 2. $Ga^{3d}_{130}/As^{3d}_{130}$ core-level intensity ratio relative to cleaved GaAs surface, vs Au overlayer thickness T . Each curve corresponds to a different initial Al coverage.

serve Au dispersing within the metallic Al overlayer. The curves in Fig. 2 continue to diverge monotonically for Au coverages of 100 Å.

The measured $Ga^{3d}_{130}/As^{3d}_{130}$ ratios represent elemental compositions near quasiequilibrium at room temperature. For 40 Å of Au on cleaved GaAs(110), both Ga^{3d}_{100} and As^{3d}_{100} increase with elapsed time t following the start of Au evaporation but reach constant values at $t > 500$ sec for As^{3d}_{100} and $t > 2000$ for Ga^{3d}_{100} . The Ga^{3d}_{100} increase between 500 and 2000 sec is only 10%. If one assumes a diffusion length $\alpha(D^{300K}_{As}t)^{1/2}$, the diffusion coefficient for As in Au has a lower limit of $\sim 10^{-16}$ cm² sec. Likewise D^{300K}_{Ga} is $> 2.5 \times 10^{-17}$ cm² sec⁻¹. Surface accumulation of Ga and As prevent further outdiffusion. Since core levels for each surface were measured at >2000 -sec intervals, any intensity errors due to the time sequence of SXPS measurements were small relative to Ga^{3d}_{130} and As^{3d}_{130} changes between surfaces.

Figure 3 illustrates the systematic dependence of the $Ga^{3d}_{130}/As^{3d}_{130}$ nonstoichiometry on the interfacial Al coverage. Each curve fits a $T^{1/2}$ dependence on the thickness of interfacial Al. The

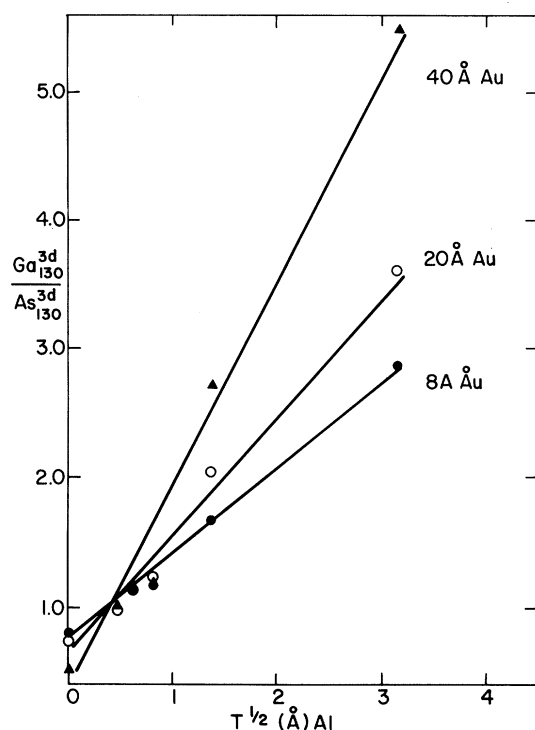


FIG. 3. $\text{Ga}^{3d}_{130}/\text{As}^{3d}_{130}$ core-level intensity ratio relative to cleaved GaAs surface, vs Al interfacial thickness T . All ratios within a given curve correspond to the same Au overlayer thickness.

absolute Ga^{3d}_{130} intensity at 40 Å is $\sim 20\text{--}40\%$ of its cleaved-surface value for all Al coverages, while the As^{3d}_{130} intensity decreases by an order of magnitude from 0 Å Al to 10 Å Al. Thus the variations in Figs. 2 and 3 are due primarily to changes in As diffusion. It is significant that the same functional dependence holds for both 8 Å Au, where most Au is observed to dissolve into the GaAs substrate, and 40 Å Au, where a thick metallic overlayer is present. Likewise, the curves in Fig. 3 exhibit the same functional dependence for both submonolayer Al coverages, where no Al-Au eutectic can form (as evidenced by the core-level spectra), and multilayer coverages, for which Au dissolving into Al is observed. Therefore, it is unlikely that any Al-Au alloy or grain boundary is directly responsible for the functional dependence in Fig. 3.

At least two models of the Au-Al/GaAs interdiffusion process can qualitatively account for the effect of monolayer interface bonding on macroscopic chemical diffusion. For example, Al atoms can act as traps for As atoms diffusing out of the GaAs lattice. A small number of Al atoms can attenuate the outdiffusing As because AlAs

exhibits a much larger heat of formation ($\Delta H_1 = -27 \text{ kcal mol}^{-1}$) than GaAs ($\Delta H_2 = -17 \text{ kcal mol}^{-1}$). The relative probability of AlAs versus GaAs bond breaking $P = \exp[-(E_1 E_2)/k_B T] = 3 \times 10^{-8}$. The attenuation should be more pronounced for diffusion involving atom transport within versus normal to the interface. Thus even monolayer Al coverages should be extremely effective as barriers to As diffusion. Alternatively, the dipole field at the intimate M-SC interface ($\sim 10^7 \text{ V/cm}$)⁴ can modify the relative anion versus cation outdiffusion, analogous to ionic motion in Mott oxidation of very thin films.⁷ For Al on GaAs (110), the -0.2-eV dipole⁹ is expected to lower (raise) the activation energy for cation (anion) motion away from the semiconductor, consistent with the relative increase of Ga to As. SXPS measurements for Au-Al/CdS interfaces also display systematic modulation which is consistent with this model. In this case the Al-CdS(1010) dipole is $+0.2 \text{ eV}$,¹⁰ and Al atoms at Au-CdS(1010) interfaces decrease the $\text{Cd}^{4d}_{95}/\text{S}^{2p}_{200}$ ratio.¹¹ This contrast between GaAs and CdS interdiffusion may result from extended field regions near the M-SC interface which contribute to the overall Schottky barriers with opposite sign.¹⁰ We are now investigating the functional dependence of these mechanisms on interface Al concentration.

The modulation of interdiffusion by Al (reactive) monolayers at both GaAs and CdS interfaces with Au (unreactive) demonstrates a general and systematic dependence of semiconductor outdiffusion, defect formation, and thereby SB formation on interface chemical reactivity.^{4,10} M-SC interdiffusion can occur at the initial stages of SB formation, and its extreme sensitivity to monolayer interfacial bonding coincides with the dramatic barrier formation observed for metal monolayers on semiconductors.^{3-5,9} The phenomena described here should also prove useful in controlling the stoichiometry of outdiffused semiconductor species. Thus, Chang, Chang, and Sheng have passivated GaAs surface by altering the stoichiometry of oxide grown between the semiconductor and a 50–100 Å Al overlayer.¹² Analogous to the ultrathin results here, the “thick” Al film retards As outdiffusion. Furthermore our results show that a wide range of chemical compositions and associated properties can be achieved via reactive atomic layers at M-SC interfaces.

Partial support by the National Science Foundation (Grant No. DMR-78-2205) is acknowledged. We thank John H. Weaver for his collaboration in the experimental work and the staff of the Syn-

chrotron Radiation Center (funded by the National Science Foundation under Grant No. DMR-74-15089) for their cooperation. We also thank Harvey Scher for valuable discussions.

¹*Thin Films—Interdiffusion and Reaction*, edited by J. M. Poate, K. N. Tu, and J. W. Mayer (Wiley-Interscience, New York, 1978).

²S. Guha, B. M. Arora, and V. P. Salvi, *Solid State Electron.* **20**, 431 (1977); A. K. Sinha and J. M. Poate, *Appl. Phys. Lett.* **23**, 666 (1973).

³G. Margaritondo, J. E. Rowe, and S. B. Christman, *Phys. Rev. B* **14**, 5396 (1976); J. E. Rowe, G. Margaritondo, and S. B. Christman, *Phys. Rev. B* **15**, 2195 (1977).

⁴L. J. Brillson, *Phys. Rev. Lett.* **40**, 260 (1978);

L. J. Brillson, *J. Vac. Sci. Technol.* **15**, 1378 (1978).

⁵I. Lindau, P. W. Chye, C. M. Garner, P. Pianetta, and W. E. Spicer, *J. Vac. Sci. Technol.* **15**, 1332 (1978); P. W. Chye, I. Lindau, P. Pianetta, C. M. Garner, C. Y. Su, and W. E. Spicer, *Phys. Rev. B* **18**, 5545 (1978).

⁶L. J. Brillson, R. S. Bauer, R. Z. Bachrach, and G. Hansson, *Appl. Phys. Lett.* **36**, 326 (1980).

⁷N. Cabrera and N. F. Mott, *Rep. Prog. Phys.* **12**, 163 (1948-49).

⁸I. Lindau and W. E. Spicer, *J. Electron Spectrosc.* **3**, 409 (1974).

⁹L. J. Brillson, R. Z. Bachrach, R. S. Bauer, and J. C. McMenamin, *Phys. Rev. Lett.* **42**, 397 (1979).

¹⁰L. J. Brillson, *J. Vac. Sci. Technol.* **16**, 1137 (1979).

¹¹L. J. Brillson, G. Margaritondo, and N. G. Stoffel, to be published.

¹²R. P. H. Chang, C. C. Chang, and T. T. Sheng, *Appl. Phys. Lett.* **30**, 657 (1977).

Elastic Relaxation Associated with the Formation and Motion of Schottky Defects in Ionic Crystals

G. A. Samara

Sandia Laboratories, Albuquerque, New Mexico 87185

(Received 26 December 1979)

Present results on CsCl-type and earlier work on NaCl-type solid ionic conductors have indicated that the relaxation of the lattice associated with vacancy formation is outward (i.e., the formation volume is greater than the molar volume). This is in qualitative disagreement with available theoretical calculations which show that the relaxation should be inward for all models of ionic vacancies investigated.

Studies of the combined effects of hydrostatic pressure and temperature on the ionic conductivities of the thallos halides (TlCl and TlBr) and of caesium chloride (CsCl) have allowed determination of the lattice volume relaxations and energies associated with the formation and motion of Schottky defects in these crystals. A particularly important result reported in this Letter is the finding that for these CsCl-type crystals the relaxation of the lattice associated with vacancy formation is *outward* (i.e., the formation volume is greater than the molar volume). While this appears to be the first such result on any crystals having the CsCl structure, earlier studies^{1,2} on ionic crystals having the NaCl structure have yielded a similar result. This *outward* relaxation thus appears to be a general result for ionic crystals of both the NaCl and CsCl types (and probably of other ionic lattice types), and it is in qualitative disagreement with theoretical calculations which show that the relaxation should be *inward* (i.e., the formation volume is less than the

molar volume) for all models of ionic vacancies investigated.¹ Resolution of this discrepancy is very important since it relates directly to our understanding of the nature of forces in simple ionic crystals.

There is considerable interest in the investigation of the relaxation of ions around defects. The determination of the activation volume for the formation and motion of lattice defects from pressure studies of diffusion and/or ionic conductivity is one of the most direct means for studying this relaxation.^{1,2} For the NaCl structure all model calculations that have been done predict an *inward* lattice relaxation for vacancies, whereas pressure results (on alkali halides) yield a relatively large *outward* relaxation.^{1,2} This disagreement is not understood. It is of much interest to examine the situation for other ionic crystal types. This interest motivated the present work on the CsCl structure. There has been relatively little work on ionic transport and the defect nature in ionic crystals having the CsCl structure